

## The precise determination of $\Re(\varepsilon'/\varepsilon)$

M.Cirilli <sup>a</sup>

*University of Rome and INFN, I-00185, Rome, Italy*

*Abstract.*  $\mathcal{CP}$  violation in the neutral kaon system is known to be dominated by the mixing of  $K^0$  and  $\bar{K}^0$ . Direct  $\mathcal{CP}$  violation in the 2 pion decays of neutral kaons has been a controversial subject over the last decade. A strong experimental effort has been devoted to the precise measurement of the direct  $\mathcal{CP}$  violation parameter  $\Re(\varepsilon'/\varepsilon)$ . After 10 years of detector development, data collection and analysis, the NA48 experiment at CERN and the KTeV experiment at Fermilab have now established direct  $\mathcal{CP}$  violation as a fact. Both KTeV and NA48 use the same experimental principle, measuring the double ratio of long lived and short lived neutral kaons to two charged and two neutral pions. However, their experimental and analysis techniques differ in important ways, and I will extensively discuss the two approaches. I will also present the latest results on  $\Re(\varepsilon'/\varepsilon)$  from both experiments, which were announced just a few months ago.

### 1 Introduction

The violation of  $\mathcal{CP}$  symmetry was first reported in 1964 by J.H. Christenson, J.W. Cronin, V. Fitch and R. Turlay, who detected a clean signal of  $\mathcal{CP}$  violating  $K_L^0 \rightarrow \pi^+ \pi^-$  decays [1].  $\mathcal{CP}$  conservation implies that the  $K_S^0$  and  $K_L^0$  particles are pure  $\mathcal{CP}$  eigenstates and that  $K_L^0$  decays only into  $\mathcal{CP} = -1$  and  $K_S^0$  into  $\mathcal{CP} = +1$  final states. The observed signal of the forbidden  $K_L^0 \rightarrow \pi\pi$  decays ( $\mathcal{CP} = +1$ ) indicates that  $\mathcal{CP}$  is not a conserved symmetry.

$\mathcal{CP}$  violation can occur via the mixing of  $\mathcal{CP}$  eigenstates, called *indirect*  $\mathcal{CP}$  violation, represented by the parameter  $\varepsilon$ .  $\mathcal{CP}$  violation can also occur in the decay process itself, through the interference of final states with different isospins. This is represented by the parameter  $\varepsilon'$  and is called *direct*  $\mathcal{CP}$  violation. L. Wolfenstein in 1964 [2] proposed a super-weak force responsible for  $\Delta S = 2$  transitions, so that all observed  $\mathcal{CP}$  violation phenomena come from mixing and  $\varepsilon' = 0$ . In 1973, Kobayashi and Maskawa proposed a matrix representation of the coupling between fermion families [3]. In the case of three fermion generations, both direct and indirect  $\mathcal{CP}$  violation are naturally accommodated in their model, via an irreducible phase.

The parameters  $\varepsilon$  and  $\varepsilon'$  are related to the amplitude ratios

$$\eta_{+-} = \frac{A(K_L^0 \rightarrow \pi^+ \pi^-)}{A(K_S^0 \rightarrow \pi^+ \pi^-)} = \varepsilon + \varepsilon'$$

and

$$\eta_{00} = \frac{A(K_L^0 \rightarrow \pi^0 \pi^0)}{A(K_S^0 \rightarrow \pi^0 \pi^0)} = \varepsilon - 2\varepsilon'$$

---

<sup>a</sup>e-mail: Manuela.Cirilli@cern.ch

which represent the strength of the  $\mathcal{CP}$  violating amplitude with respect to the  $\mathcal{CP}$  conserving one, in each mode. By the mid-1970s, experiments had demonstrated that  $\mathcal{CP}$  violation in the neutral kaon system is dominated by mixing, with the limit  $\Re(\varepsilon'/\varepsilon) \leq 10^{-2}$  [4]. On the other hand, theoretical work showed that direct  $\mathcal{CP}$  violation in the Standard Model could be large enough to be measurable [5]. This stimulated experimental effort with sophisticated detectors to measure  $\Re(\varepsilon'/\varepsilon)$ . The first evidence for the existence of a direct component of  $\mathcal{CP}$  violation was published in 1988 [6]. In 1993, two experiments published their final results without a conclusive answer on the existence of this component. NA31 [7] measured  $\Re(\varepsilon'/\varepsilon) = (23.0 \pm 6.5) \times 10^{-4}$ , indicating a  $3.5\sigma$  effect. The result of E731 [8],  $\Re(\varepsilon'/\varepsilon) = (7.4 \pm 5.9) \times 10^{-4}$ , was instead compatible with no effect.

The controversial results from NA31 and E731 called for the realization of more precise experiments, to measure  $\Re(\varepsilon'/\varepsilon)$  with a precision of  $\mathcal{O}(10^{-4})$ . Presently, there are three experiments in different laboratories working on the precise measurement of  $\Re(\varepsilon'/\varepsilon)$ : two of these, namely NA48 [9] at CERN and KTeV [10] at Fermilab, represent the “evolution” of NA31 and E731 respectively; the third one is KLOE [11] at the Laboratori Nazionali di Frascati and its conceptual design is radically different from the other experiments.

This paper is devoted to a comparative presentation of KTeV and NA48, since these experiments have already published results. Detector designs and analysis techniques will be discussed, together with the results announced just recently from these two collaborations [12] [13].

## 2 The experimental method

Experimentally, it is convenient to measure the double ratio  $\mathcal{R}$ , which is related to the ratio  $\Re(\varepsilon'/\varepsilon)$ :

$$R = \frac{\Gamma(K_L^0 \rightarrow \pi^0 \pi^0)}{\Gamma(K_S^0 \rightarrow \pi^0 \pi^0)} / \frac{\Gamma(K_L^0 \rightarrow \pi^+ \pi^-)}{\Gamma(K_S^0 \rightarrow \pi^+ \pi^-)} \approx 1 - 6 \times \Re(\varepsilon'/\varepsilon) \quad (1)$$

The double ratio  $\mathcal{R}$  is experimentally measured by *counting* the number of decays detected in each of the four modes in equation 1. The statistical error is dominated by the events collected in the most suppressed decay, namely  $K_L^0 \rightarrow \pi^0 \pi^0$  ( $BR \sim 0.09\%$ ). The value  $\mathcal{R}_{true}$  is then deduced correcting the measured value  $\mathcal{R}_{meas}$  for the kaon beam fluxes, detector acceptances, trigger efficiencies, backgrounds evaluations, etc., i.e. for all the possible biases in the counting process. It is now evident that the difficulty of  $\Re(\varepsilon'/\varepsilon)$  measurements lies in the necessity to disentangle the  $\mathcal{CP}$  violating  $K_L^0$  modes from the dominant environment of  $\mathcal{CP}$  conserving 3-body decays of both  $K_L^0$  and  $K_S^0$ .

## 2.1 Advantages of the double ratio technique

The main advantage of the double ratio measurement, when performed under the adequate data taking conditions, is that the corrections to  $\mathcal{R}_{meas}$  can cancel out at first order. Let us consider the beam fluxes and trigger/reconstruction efficiencies corrections as an example:

- **Beam fluxes:** the knowledge of the kaon flux in the  $K_S^0$  and  $K_L^0$  beams is a priori needed for normalization purposes. However, if the charged and neutral decay modes of either the  $K_S^0$  or the  $K_L^0$  are simultaneously collected, then the ratio of  $\pi^+\pi^-$  and  $\pi^0\pi^0$  events in each beam is independent from the absolute flux. Hence, under these conditions, beam fluxes cancel out in the double ratio at first order.
- **Efficiencies:** the trigger scheme is conceived to minimise any loss of good events. However, a small correction usually has to be applied to  $\mathcal{R}_{meas}$  to account for trigger inefficiencies. A first order cancellation of this correction can be achieved for the charged/neutral trigger efficiency if both  $K_L^0$  and  $K_S^0$  decays into the charged/neutral final state are simultaneously collected. The same principle also holds for any instability of a given detector, which could affect the reconstruction efficiency of the charged or neutral modes.

The best strategy to exploit the cancellation of eventual biases is to collect all the four modes simultaneously. This allows to evaluate only second order effects to get the true value  $\mathcal{R}_{true}$  from  $\mathcal{R}_{meas}$ . Even in this ideal situation, there will still be some leftover corrections that do not cancel out. This is the case for the physical background, which comes only from  $K_L^0$  decays and is clearly final-state-dependent. Also, acceptance corrections do not a priori cancel out in the four modes: this is related to the huge lifetime difference between  $K_L^0$  and  $K_S^0$ , which causes very different longitudinal decay vertex distributions for the two beams, and to the different topologies of  $\pi^0\pi^0 \rightarrow 4\gamma$  and  $\pi^+\pi^-$  events. Both the physical background and the acceptance correction must be carefully studied, and different solutions can be envisaged to handle them.

All the above considerations have been thoroughly taken into account while conceiving KTeV and NA48. The design of the experiments and the analysis methods focus on making the inevitable systematic biases in the event counting symmetric between at least two of the four components of the double ratio. In this way, most of the important systematic effects cancel to first order, and only the differences between two components need to be considered in detail in the analysis. This allows the systematic uncertainties to be kept sufficiently low.

### 3 KTeV and NA48: overview

Both KTeV and NA48 are fixed target experiments designed to simultaneously collect all the four decay modes in 1. Measuring  $\Re(\varepsilon'/\varepsilon)$  to a precision of  $\sim 10^{-4}$  requires several millions of  $K_L^0$  and  $K_S^0 \rightarrow \pi\pi$  decays: this implies taking data with high-intensity kaon beams and running for several years to achieve the desired statistics. A number of challenges had to be faced during the design phase. Stable detectors were needed to sustain the long data taking periods. The trigger electronics had to be fast enough to cope with the high flux of particles in the decay region and a powerful data acquisition was needed to handle the high trigger rates. The overwhelming  $3\pi^0$  background set the requirement of an extremely precise electromagnetic calorimeter. The whole detector had to be radiation-hard, to cope with the beam intensities. Long R&Ds were necessary to meet these very demanding requirements, and this effort has also been profitable in view of future experiments in high-intensity environments (*e.g.*, the Tevatron and LHC).

KTeV collected  $\sim 7\text{M}$  events in the most suppressed channel  $K_L^0 \rightarrow \pi^0\pi^0$  during the 96, 97 and 99 runs. A first  $\Re(\varepsilon'/\varepsilon)$  measurement [14] was announced in February, 1999, based on 10% of the total sample. In June, 2001, KTeV presented a new result on the 97 data sample, together with an update of the already published result: the combined measurement [13] is obtained from  $\sim 50\%$  of the available data. NA48 took data in 97, 98 and 99, collecting almost 4M events in the neutral  $K_L^0$  decay mode. The first  $\Re(\varepsilon'/\varepsilon)$  measurement [15] was reported in June, 1999, and was based on the statistics collected during the 97 run; a preliminary result on the 98 sample was presented in February, 2000. The final result on the 98 and 99 data [12] was announced in May, 2001. A slight increase in statistics for NA48 is expected from the data collected in the 2001 run.

#### 3.1 KTeV: Detector and beam lines

A schematic view of KTeV detectors and beams is shown in figure 1. KTeV exploits the 800 GeV proton beam delivered by the Tevatron: two nearly parallel kaon beams are produced by the protons hitting a 50 cm long beryllium target at 4.8 mrad angle. The beams are cleaned up and let fly for roughly 120 m, so that only the  $K_L^0$  component survives. The beams direction defines the longitudinal  $z$  axis. The decay region begins at the end of the last collimator; here the two beams are 10 cm apart, and one of them hits a 1.8 m long regenerator made of plastic scintillators. The regenerator beam is a coherent superposition  $K_L^0 + \rho K_S^0$  of long- and short-lived kaons. The regenerated fraction  $\rho$  is proportional to the amount of matter traversed by the previously pure  $K_L^0$  beam, and its value 0.03 is sufficient to ensure that the regenerator  $2\pi$  decays are dominated by  $K_S^0 \rightarrow \pi\pi$ . The regenerator technique ensures that

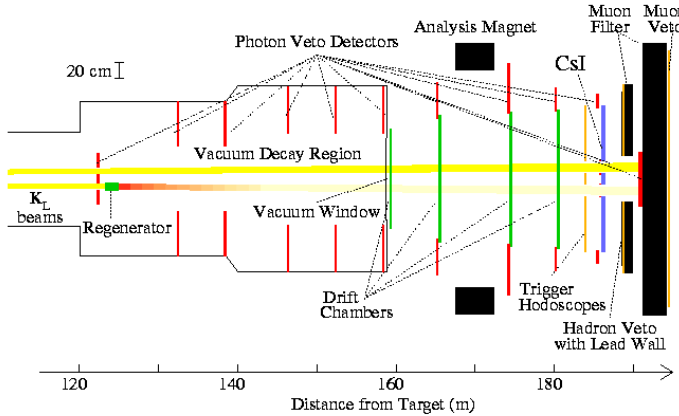


Figure 1: Top view of KTeV detector and beam lines.

the  $K_S^0$  are produced with an energy spectrum similar to that of  $K_L^0$ . The decay region extends up to 159 m from the primary target.

A distinctive feature of KTeV is the fact that the two beams are parallel and hit the detectors at separate points (left and right). This allows to easily identify  $K_L^0$  and  $K_S^0$  decays reconstructing the transverse decay vertex position and comparing it with the known regenerator position. The regenerator is fully instrumented, and switches beam line once per minute, in order to reduce the effects of possible left-right asymmetries of the detectors.

Charged kaon decays are detected by a spectrometer consisting of a central magnet with a 411 MeV/c kick in the horizontal plane and of four drift chambers with wires along the  $x$  and  $y$  directions. The spectrometer has a position resolution of  $100\mu\text{m}$  and a momentum resolution  $\sigma_p/p = 0.17\% \oplus [0.008 \times p]\%$ , where  $p$  is in  $\text{GeV}/c$  units.

Neutral decays are detected by a crystal calorimeter [16] consisting of 3100 pure CsI blocks. The crystals cover  $27X_0$  in length (50 cm) and have a transverse section of  $2.5 \times 2.5\text{cm}^2$  in the central region, where the density of photons is higher; in the outer region of the calorimeter, the granularity is of  $5 \times 5\text{cm}^2$ . The main advantage of this calorimeter lies in its excellent stochastic term in the energy resolution, which allows to reach an overall resolution of 0.7% for a 15 GeV photon (as shown in figure 2 left). The longitudinal light collection is equalised within 5% by means of a meticulous crystal wrapping. In addition, the stability of the response for each crystal is continuously checked using a  $\text{Cs}^{137}$  source for calibration. The overall energy response is linear within 0.4%.

### CsI Calorimeter Performance

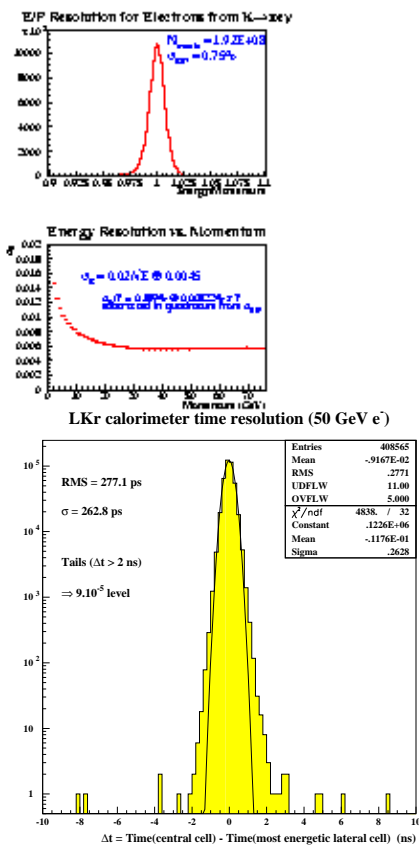


Figure 2: Performances of KTeV CsI crystal calorimeter (left) and of the NA48 LKr ionization calorimeter (right)

The main apparatus is surrounded by circular vetoes to detect escaping photons, and a muon veto placed at the end of the line is used to identify  $K_{\mu 3}$  decays.

### 3.2 NA48: Detector and beam lines

A schematic view of the NA48 beam lines is given in figure 3. The primary 450 GeV proton beam is delivered from the SPS and impinges on a 40 cm beryllium target with an incidence angle of 2.4 mrad relative to the  $K_L^0$  beam axis. The charged component of the outgoing particles is swept away by bending magnets, while the neutral beam component passes through three stages of collimation. The fiducial region starts at the exit of the “final” collimator, 126 m downstream of the target. At this point, the neutral beam is dominated by long-lived kaons. The non-interacting protons from the  $K_L^0$  target are directed onto a mechanically bent mono-crystal of silicon. A small fraction ( $10^{-5}$ ) of protons satisfies the conditions for channelling and is deflected following the crystalline planes. Use of the crystal allows a deflection of 9.6 mrad to be obtained in only 6 cm length, corresponding to a bending power of 14.4 Tm. The transmitted protons pass through the tagging station (or *tagger*), which precisely registers their time of passage. They are then deflected back onto the  $K_L^0$  beam axis, transported through a series of quadrupoles and finally directed to the  $K_S^0$  target (same size as  $K_L^0$ ) located 72 mm above the  $K_L^0$  beam axis. A combination of collimator and sweeping magnet defines a neutral beam at 4.2 mrad to the incoming protons. The decay spectrum of kaons at the exit of the collimator is similar to that in the  $K_L^0$  beam, with an average energy of 110 GeV. The fiducial region begins 6 m downstream of the  $K_S^0$  target, such that decays are dominated by short lived particles. At this point, the  $K_S^0$  and  $K_L^0$  beams emerge from the aperture of the final collimators into the common decay region. The whole  $K_S^0$  target and collimator system is aligned along an axis pointing to the centre of the detector 120 m away, such that the two beams intersect at this point with an angle of 0.6 mrad.

Since the two beams are not separated at the detector position, as it is in KTeV, the identification of  $K_L^0$  and  $K_S^0$  decays must be accomplished in a different way. This is done using the tagging station, which consists of two scintillator ladders, crossing the beam horizontally and vertically. The coincidence between the proton time and the event time in the detectors assigns the decay to the  $K_S^0$  beam. Two close pulses can be resolved down to 4–5 ns.

The reconstruction of charged decays is performed by a magnetic spectrometer, with a central magnet giving a 250 MeV/c transverse kick and four chambers with plane wires oriented along four different directions  $x$ ,  $y$ ,  $u$  and  $v$ . The redundancy of the planes allows to resolve the possible track ambiguities.

NA48 has chosen a liquid Krypton ionization calorimeter with a depth of  $27X_0$ , corresponding to 125 cm. The read-out is performed by Cu-Be-Co rib-

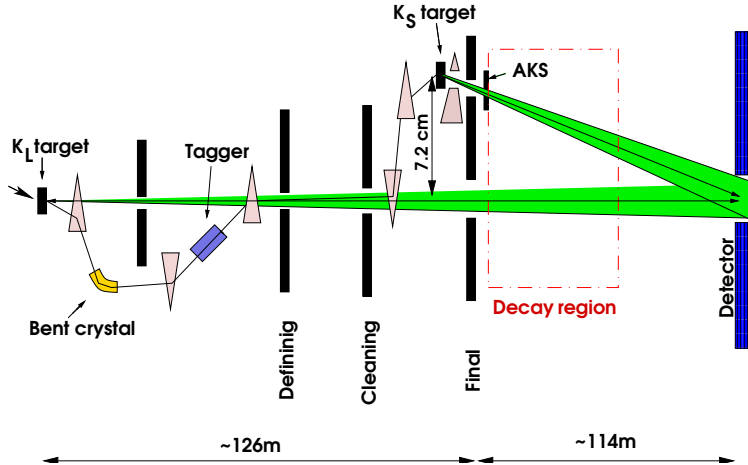


Figure 3: Schematic view of NA48 beam lines (not to scale).

bons defining  $\sim 13\,000$  cells, in a structure of longitudinal projective towers pointing to the centre of the decay region. The cross section of a cell is about  $2\text{ cm} \times 2\text{ cm}$ , and the electrodes are guided longitudinally through precisely machined holes in five spacer plates. The planes also apply a  $\pm 48$  mrad zig-zag to the electrodes, in order to maintain the mechanical stability and to decrease the sensitivity of the energy resolution to the impact position. Good energy response is further guaranteed by the initial current readout technique which also provides a high rate capability. The overall energy resolution is 1.5% at 10 GeV. The energy response is linear to about 0.1% in the range 5–100 GeV. A precise time measurement is mandatory for the NA48 calorimeter, since it must be used together with the proton time from the tagger to distinguish  $K_S^0$  from  $K_L^0$ . The neutral event time is reconstructed with a precision of  $\sim 220$  ps.; tails coming from misreconstructed times are below the level of  $10^{-4}$  (see figure 2 right).

A muon veto system is used to reject muons from  $K_{\mu 3}$  decays.

#### 4 KTeV and NA48: analysis techniques

Once the events are collected, all corrections that do not cancel in the double ratio must be applied. The long list of residual effects that must be studied includes physical backgrounds,  $K_S^0 - K_L^0$  misidentifications, trigger efficiencies, Monte Carlo correction, geometrical acceptances, detector biases (calorimeter energy scale, drift chamber alignment, etc.), accidental effects. In the following,

I will focus on just a few of these effects, highlighting the important differences between KTeV and NA48 approach.

#### 4.1 Selection of the $\pi^+\pi^-$ sample

Both experiments use the magnetic spectrometer to reconstruct the kaon mass, vertex and momentum. The resolution on the kaon mass in the charged mode is 1.5 MeV in KTeV and 2.5 MeV in NA48. The better KTeV resolution is due to the higher transverse kick of their magnet and to the choice of having only  $x$  and  $y$  planes in the drift chambers. This choice implies lighter chambers with respect to NA48, and so a lower multiple scattering term in the resolution. However, having only two views reduces the capability of resolving ambiguities in the track reconstruction: for this reason, KTeV needs additional information from the calorimeter to perform a reliable reconstruction of  $\pi^+\pi^-$  events.

Background to $K^0 \rightarrow \pi^+\pi^-$			
Background source	KTeV (vac)	KTeV (reg)	NA48 $K_L^0$
$K_{\mu 3} + K_{e3}$	$0.9 \times 10^{-3}$	$0.03 \times 10^{-3}$	$1.69 \times 10^{-3}$
Collimator scatt.	$0.10 \times 10^{-3}$	$0.10 \times 10^{-3}$	-
Regenerator scatt.	-	$0.73 \times 10^{-3}$	-

Table 1: Summary of background fractions in the charged mode.

$K_{\mu 3}$  decays are rejected using the identified muon in the dedicated vetoes, while electrons from  $K_{e3}$  events are identified comparing the track momentum in the spectrometer with the corresponding energy in the calorimeter. Additional cuts are imposed on the reconstructed mass and transverse momentum. The leftover background contributions are then evaluated studying high-statistics samples of the identified 3-body decays. The background fractions in the two experiments are summarized in table 1, including the components due to scattering in the collimator and (only for KTeV) regenerator.

#### 4.2 Selection of the $\pi^0\pi^0$ sample

Both experiments base the reconstruction of neutral events on the information from the electromagnetic calorimeter. In addition to the energies and positions of the four photons, a mass constraint must be imposed in order to reconstruct the decay vertex position. KTeV method imposes the  $\pi^0$  mass to all photon pairs combinations, computing the vertex position for each pairing; only the two closest solutions are kept, and they are combined to produce the most probable value for the kaon decay vertex. NA48 method imposes the kaon invariant mass on the  $4\gamma$  event, thus constraining the decay vertex position. The two  $pio$  are reconstructed choosing the best of all the possible pairings between the photons.

Background to $K^0 \rightarrow \pi^0\pi^0$			
Background source	KTeV (vac)	KTeV (reg)	NA48 $K_L^0$
$K_L^0 \rightarrow 3\pi^0$	$1.1 \times 10^{-3}$	$0.3 \times 10^{-3}$	$0.59 \times 10^{-3}$
Collimator scatt.	$1.2 \times 10^{-3}$	$0.9 \times 10^{-3}$	$0.96 \times 10^{-3}$
Regenerator scatt.	$2.5 \times 10^{-3}$	$11.3 \times 10^{-3}$	-
Regenerator had. int	-	$0.1 \times 10^{-3}$	-

Table 2: Summary of background fractions in the neutral mode.

Both experiment define a  $\chi^2$  variable that states the compatibility of each event with the  $K^0 \rightarrow \pi^0\pi^0$  hypothesis. Background events from  $K_L^0 \rightarrow 3\pi^0$  decays with lost or merged photons have a high value of the  $\chi^2$  and are rejected. The amount of remaining background is evaluated from a high-statistic sample of  $3\pi^0$  events. Background fractions for KTeV and NA48 are summarized in table 2.

#### 4.3 $K_S^0$ and $K_L^0$ identification

As already described in sections 3.1 and 3.2, the two experiments use different techniques to distinguish  $K_S^0$  from  $K_L^0$ . KTeV takes advantage of having two parallel beams: the 10 cm separation allows to disentangle  $K_S^0$  and  $K_L^0$  by looking at the reconstructed decay vertex position in the transverse plane, in the case of charged events. In the case of neutral events, the energy centroid of the four photons is used, as shown in figure 4 left. The halo surrounding one of the two beams is due to events scattered in the regenerator before decaying: this effect is accurately studied in the  $p_T^2$  distribution of charged events, and is then introduced into a detailed simulation to evaluate the contribution in the neutral case.

NA48 uses the tagging method: a decay is identified as  $K_S^0$  if its event time is within a  $\pm 2$  ns coincidence with a proton time measured by the tagger. The principle can be clearly illustrated for charged events, which can be identified as  $K_S^0$  or  $KL$  also on the basis of the vertical separation between the two beams at the drift chamber position. This is shown in figure 4 right, where the difference between the event time and the time of the nearest proton in the tagger is plotted. It is evident that the inefficiencies in identifying true  $K_S^0$  decays is very small ( $10^{-4}$  level). On the other hand, there is a sizeable mistagging probability in the case of  $K_L^0$ : the high rate of events in the  $K_L^0$  beam causes accidental coincidences, and it turns out that  $\sim 10\%$  of the true  $K_L^0$  events are misidentified as  $K_S^0$ . The final data samples are corrected for both inefficiency and accidental tagging.

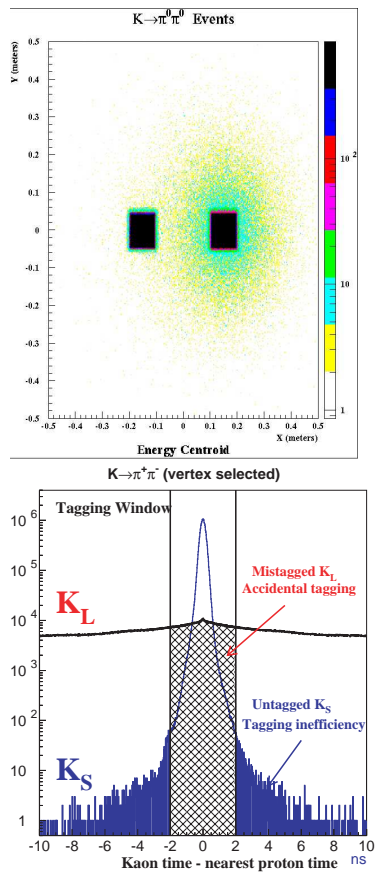


Figure 4: Procedure for  $K_S^0$  and  $K_L^0$  identification in KTeV (left) and NA48 (right).

#### 4.4 From event counting to $\mathcal{R}$

Having identified  $K_S^0$  and  $K_L^0$ , as well as charged and neutral decays, both experiments end up with four samples of events. In the case of KTeV, the samples correspond to the Vacuum beam ( $K_L^0$  decays) and to Regenerator beam (mostly  $K_S^0$ ) into  $\pi^+\pi^-$  and  $\pi^0\pi^0$  final modes. The striking difference in the decay vertex distributions for  $K_S^0$  and  $K_L^0$  translates in a large acceptance correction, which therefore must be precisely known. The correction is implemented using a highly detailed Monte Carlo simulation which includes all known effects, as trigger and detector efficiencies, regeneration,  $K_S^0 - K_L^0$  interference, detector apertures, etc. The value of  $\Re(\varepsilon'/\varepsilon)$  is then obtained fitting the data in 10 GeV bins in the kaon energy, in order to minimise residual differences in the energy spectra.

NA48 has two charged/neutral samples of tagged events (essentially  $K_S^0$ ) and two other charged/neutral samples of untagged events ( $K_L^0$  with a  $\sim 10\%$  contamination of  $K_S^0$ ). All samples are corrected for mistagging and trigger inefficiencies. The final result is computed by dividing the data into 20 bins of kaon energy from 70 to 170 GeV, and calculating the double ratio for each bin. To cancel the contribution from the different lifetimes to the acceptance,  $K_L^0$  events are weighted with the  $K_S^0$  lifetime as a function of the reconstructed proper decay time. After weighting, the  $K_L^0$  and  $K_S^0$  decay distributions become nearly identical and the size of the acceptance correction is drastically reduced. The weighting technique avoids the need of an extremely sophisticated simulation, although it results in a  $\sim 35\%$  increase of the statistical error on  $R$ . All corrections are applied to each bin separately, and the results are averaged using an unbiased estimator.

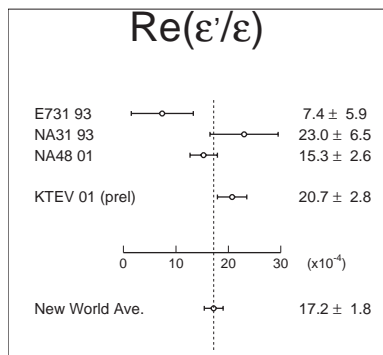


Figure 5: Summary of results on  $\Re(\varepsilon'/\varepsilon)$ .

## 5 Results from KTeV and NA48

The latest results from KTeV [13] and NA48 [12] are summarized in figure 5, together with the final results from NA31 and E731. The new world average value of  $\Re(\varepsilon'/\varepsilon)$  is  $(17.2 \pm 1.8) \times 10^{-4}$ . This result confirms the existence of direct  $\mathcal{CP}$  violation in the neutral kaon system. Whether the measured size of  $\Re(\varepsilon'/\varepsilon)$  is compatible with Standard Model expectations or is a hint that new physics is at work, this is still matter of debate: theoretical calculations suffers from big uncertainties in the determination of the hadronix mass matrix elements, thus their predictive power on  $\varepsilon'/\varepsilon$  is rather poor.

Establishing beyond doubt the existence of the direct  $\mathcal{CP}$  violation mechanism has been a long experimental adventure. Both KTeV and NA48 have still other data samples to analyse, and hopefully KLOE will provide also its measurement of  $\Re(\varepsilon'/\varepsilon)$  with a different method. We recently witnessed the first observation of  $\mathcal{CP}$  violation in a system other than the neutral kaon system, namely in  $B^0 - \overline{B}^0$  oscillations.  $\mathcal{CP}$  violation studies are also being performed in the sector of B and K rare decays. Considering all these constraints together, there is reasonable hope that a deeper understanding of the  $\mathcal{CP}$  violation mechanism will be achieved in the forthcoming years.

## Acknowledgements

I would like to warmly thank the organisers of the 10<sup>th</sup> Lomonosov Conference on Elementary Particle Physics for the interesting meeting.

## References

- [1] J.H. Christenson et al., Phys. Rev. Lett. **13**, 138 (1964)
- [2] L. Wolfenstein, Phys. Rev. Lett. **13**, 562 (1964).
- [3] M. Kobayashi and K. Maskawa, Prog. Theor. Phys. **49**, 652 (1973).
- [4] M. Holder et al., Phys. Lett. B **40**, 141 (1972); M. Banner et al., Phys. Rev. Lett. **28**, 1957 (1972).
- [5] J. Ellis, M.K. Gaillard and D.V. Nanopoulos, Nucl. Phys. B **109**, 213 (1976); F.J. Gilman and M.B. Wise, Phys. Lett. B **83**, 83 (1979).
- [6] H. Burkhardt et al., Phys. Lett. B **206**, 169 (1988).
- [7] G. Barr et al., Phys. Lett. B **317**, 233 (1993).
- [8] L.K. Gibbons et al., Phys. Rev. Lett. **70**, 1203 (1993).
- [9] G. D. Barr *et al.*, CERN/SPSC/90-22 (1990).
- [10] K. Arisaka *et al.*, FN-580 (1992).
- [11] The KLOE Collaboration, LNF-93/002 (1993).
- [12] A. Lai *et al.* [NA48 Collaboration], CERN-EP-2001-067.

- [13] J. Graham [KTeV Collaboration], FNAL Seminar; R. Kessler, hep-ex/0110020.
- [14] A. Alavi *et. al.*, [KTeV Collaboration], Phys. Rev. Lett. **83**, 22 (1999).
- [15] V. Fanti et al., Phys. Lett. **B** 465, 335-348 (1999).
- [16] R. S. Kessler *et. al.*, Nucl. Instr. Meth. A **368**, 653 (1996).
- [17] G. Barr *et. al.*, Nucl. Instr. Meth. Phys. Res. A **370**, 413 (1996).